

EXPERIMENTAL AND FINITE ELEMENT ANALYSIS OF MULTILAYERED HONEYCOMB COMPOSITE MATERIAL SUBJECT TO STATIC LOADING

Cormos RAUL¹, Horia-Alexandru PETRESCU², Anton HADAR³

A set of four different multilayered honeycomb composite materials were created for the purpose of determine their mechanical properties under static compressive loading. Thus, the four different configurations were subjected to a specific compression test and afterwards retested, in the same manner but through numerical virtualization.

Validation of these results allows the use of such finite element models in widespread areas of engineering such as aeronautics, but not limited thereto.

Keywords: honeycomb structure, numerical virtualization, composite materials, numerical validation.

1. Introduction

Sandwich structures are composite materials with high strength and low mass. This combination of mechanical properties makes them highly used in many areas of mechanical engineering, such as: aerospace, naval and automobile industry, as well on civilian and military. The result of the usage of sandwich structures, in these areas of mechanical engineering, are stronger and lighter structural components [4, 5].

The most important industrial applications of honeycomb sandwich structures can be found in the aerospace industry. Such applications as helicopter rotor blades, hall of the aircraft, aircraft engine turbine noise reduction, or spacecraft structures represents the highest performance demanding areas where the usage of honeycomb sandwich structures is vital. A study about their applications for the Boeing 737-800 interiors is reported in [13].

L. J. Gibson [1] and J. R. Vinson [3], have demonstrated that the most important load bearing component for a statically loaded honeycomb sandwich

¹ Faculty of Applied Chemistry and Materials Science, University POLITEHNICA of Bucharest, Romania, e-mail: cormosr@yahoo.com

² Faculty of Applied Chemistry and Materials Science, University POLITEHNICA of Bucharest, Romania

³ Faculty of Applied Chemistry and Materials Science, University POLITEHNICA of Bucharest, Romania

structure is the core component. Furthermore Gibson [1] and Bruhn [7] have numerically determined the mechanical properties of the honeycomb sandwich structure based on the honeycomb cell configuration and the material used for the honeycomb core. Also, it presented that a regular cell sized honeycomb structure has isotropic mechanical properties in the tangential direction of the cell, if the cell structure is made by evenly sized cells.

The loading curve of a honeycomb core, axially loaded, is independent by the material from which the core is made, or the cell size.

The failure of honeycomb cores statically loaded on the transversal direction (bending or shear) of the cell occurs by the appearance of yield points on the intersection of the cells. In [9], the plastic collapse of inclined walls in the Y-direction due to plastic hinges formation is depicted.

For a honeycomb sandwich structure subjected to compression, the failure of the core is caused by the buckling effect of the cell walls, not by compression stress failure. An approach, based on an elasticity solution that matches the deformations of individual face-sheets, focused on the calculation of stresses and predict failure in sandwich ramp-down regions under bending loads is presented in [10].

Out-of-plane compressive tests on bare honeycombs were carried out in [17] resulting that the compressive stress increases almost linearly with the strain due to the elastic bending of the thin cell walls.

The multitudes of cores used in the sandwich structures, gives different mechanical properties alongside their thickness, for these materials. In the last decades, strong efforts have been made to develop nonconventional cores for sandwich structures. These resulted in new mechanical properties such as negative Poisson's ratio [6].

Thus, development of nonconventional sandwich structures, such as multilayered honeycomb composite materials, represents a strategic line of development in the area of future composite materials.

For mechanical applications, any load is transmitted through contact.

There is an increasing practical interest in the application of cellular materials (such as honeycombs and foams) being used in passive vehicle safety systems as crash energy absorber elements [14-16].

Analytical methods have been developed to describe the impact phenomena, for regularly sized bodies. These methods are not suited to describe the contact phenomena for bodies with highly complex contact geometry.

With the development of the finite element method (FEM) new computational methods were introduced which allow the numerical simulation of the contact phenomena for complex contact areas between bodies. One such method is the penalty method presented by P. Wriggers [2, 8], which represents the most used method for finite element simulation in contact mechanics. This

energetic method allows the determination of contact force between the two bodies, considering the elasticity of the bodies.

Tao Zhu et al. in [11] have used FEM to predict the local buckling behavior and the debonding propagation in honeycomb sandwich structures.

In order to reflect microscopic structure and deformation of the unit cell, periodic boundary conditions should be applied on unit cell, as is stated in [12], but not the case of this study due to the mesoscale of our study.

The main purpose of this article is to validate the finite element analysis of four multilayered honeycomb composite material configurations subjected to static loading, in the linear elastic domain of the material.

2. Multilayered honeycomb composite material description

The four multilayered honeycomb composite material configurations, have five layers, three laminated woven fabric layers and two honeycomb cores. Two outer face sheets are double layered woven fiberglass composites impregnated in polyester resin. The core of the composite material consists of two honeycomb layers separated by a single layered woven fiberglass sheet impregnated in polyester resin. A general image of this configurations is presented in Fig. 1. The four-multilayered honeycomb composite material configurations differ from one another, by the type of the two types of honeycomb cores used, paper and impregnated paper in polyester resin. Thus, the first one is with both honeycomb layers made of impregnated paper, the second one has the first honeycomb core made of impregnated paper and the second core made of paper, the third multilayered honeycomb composite material has the first layer made of paper, and the second layer from impregnated paper, and the fourth multilayered honeycomb composite material has both cores honeycomb layers paper.

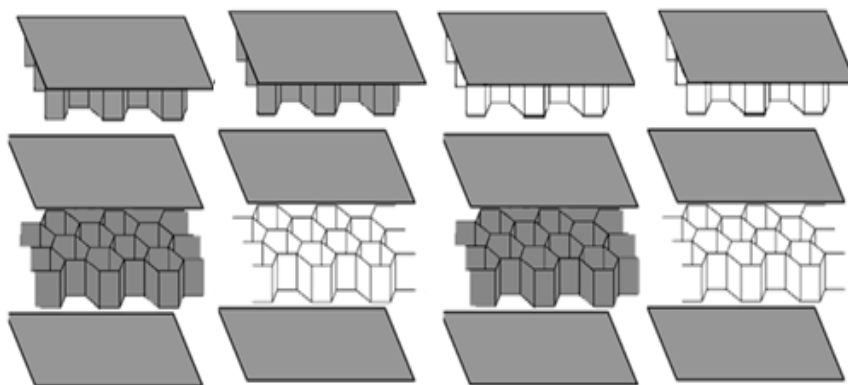


Fig. 1. Image of multilayered honeycomb composite materials configuration

3. Finite element and geometrical models

The geometrical model has three main components: the stamp, the multilayered honeycomb composite material and the lower support, Fig. 2.

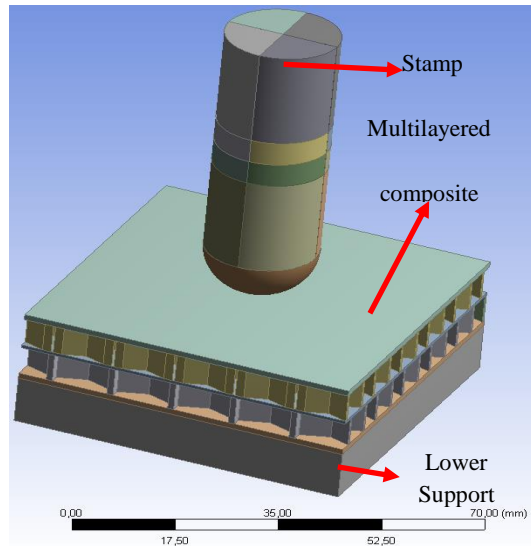


Fig. 2. Finite element model of components used in experiments

The stamp has a conical head with 20 mm in diameter. The multilayer honeycomb composite material specimen and the lower support have the dimensions of 60 x 60 mm. The thicknesses of the two honeycomb cores are 0.23 mm for the paper honeycomb core and 0.55 for the impregnated paper honeycomb core. The other geometrical dimensions, of the multilayered honeycomb composite material are presented in Fig. 3.

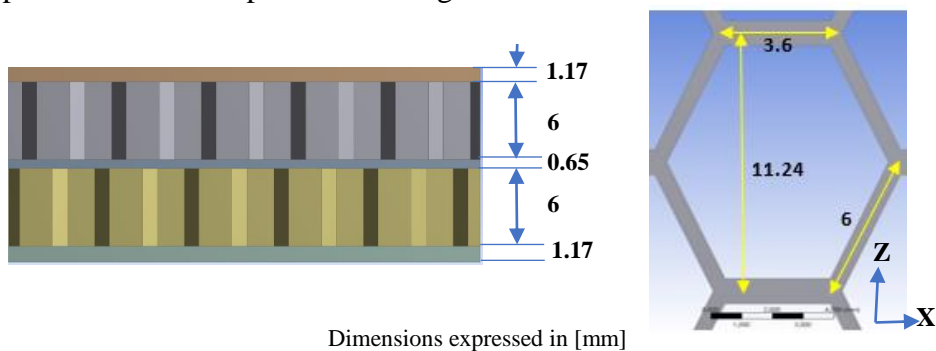


Fig. 3.a. Composite material front view

Fig. 3.b. Honeycomb core cell dimensions

Fig. 3. Honeycomb core geometry

The lower support, on which multilayered honeycomb composite material is placed, has a hole in the center of 40 mm in diameter. For these multilayered honeycomb composite materials, the position of the two honeycomb layers are not known to each other, four geometrical models were considered, based on the position of the honeycomb layers.

The first configuration has both honeycomb cores overlapped, Fig. 4.

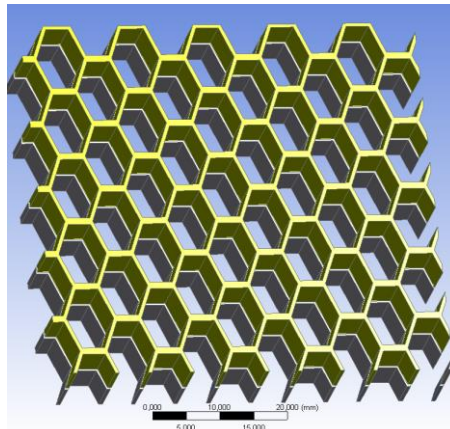


Fig. 4. First multilayered honeycomb composite material configuration

The second geometrical configuration has a 3.53 mm distance between the two cores on the X axis direction, Fig. 5.



Fig. 5. Second geometrical configuration for the multilayered honeycomb composite material

The third geometrical configuration has a distance of 5.62 mm on the Z axis direction between the two cores, Fig. 6.

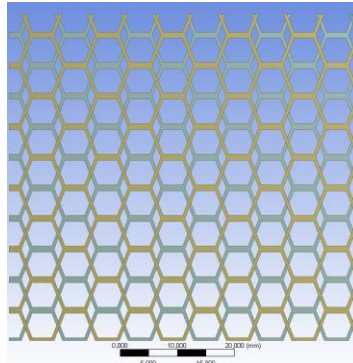


Fig. 6. Third geometrical configuration for the multilayered honeycomb composite material

The fourth geometrical configuration is made from the displacements of the two honeycomb cores in the second and third geometrical models, Fig. 7.

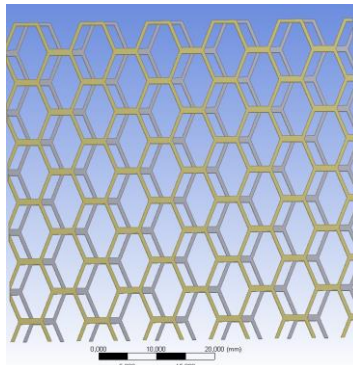


Fig. 7. Fourth geometrical configuration for multilayered honeycomb composite material

4. Material properties

The elastic properties of the materials used in the analysis are presented in the table 1. The elastic properties were obtained by tension testing. To reduce the computational power required, the elastic modulus of the composite material is computed as a mediated value between the longitudinal elastic modulus of 16954 MPa and the transversal elastic modulus, of 14684 MPa.

Table 1

Mechanical properties of materials

Material name	Young Modulus [MPa]	Poisson Ratio
Composite	15819	0.33
Paper	11511	0.2
Impregnated Paper	16357	0.35

5. Experimental testing

The experimental device used to determine the static response of the multilayered honeycomb composite materials to the given loading conditions is a universal **INSTRON 8800** of 100 kN testing machine. The experimental testing is made through applying a given displacement and registering the force obtained for the given displacement of the stamp.

For the four-multilayered honeycomb, composite material configurations the forces are taken in a number of displacement points in the linear elastic domain of the materials. For each material type three tests are made. For these tests the experimental response curves are determined for each configuration of the multilayered honeycomb composite material.

The experimental results for each of the multilayered honeycomb composite materials are presented in Figs. 8-11.

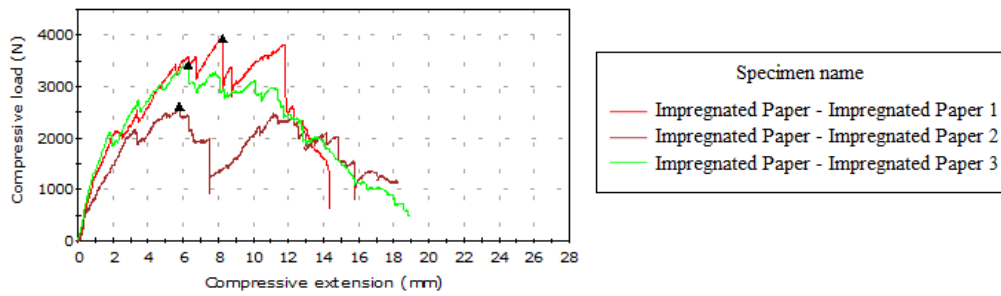


Fig. 8. First multilayered honeycomb composite material which both honeycomb cores with impregnated paper

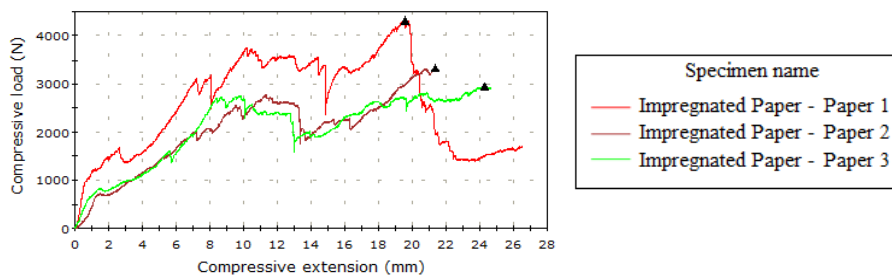


Fig. 9. Second multilayered honeycomb composite material with the first honeycomb for impregnated paper and the second one paper honeycomb core

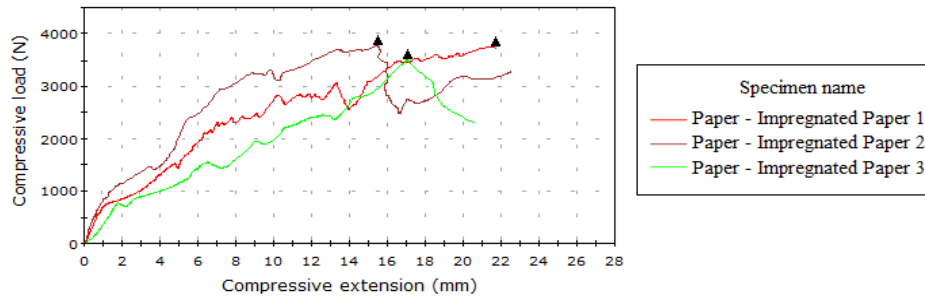


Fig. 10. Third multilayered honeycomb composite materials with the first honeycomb paper and the second one impregnated paper

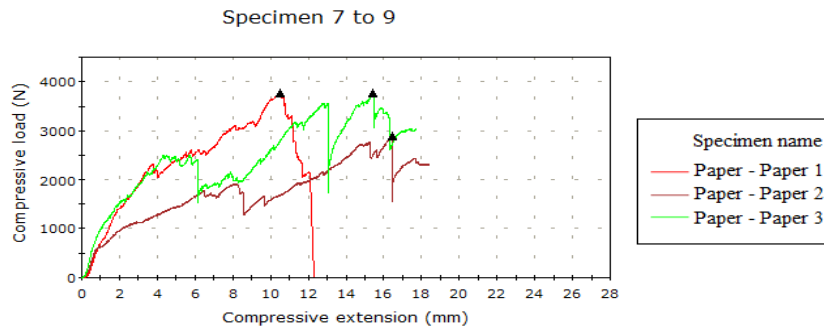


Fig. 11. Fourth Multilayered honeycomb composite materials with both honeycomb cores paper

6. Finite element analysis results

The finite element analysis was carried out in ANSYS, version 15, Static Structural module.

To validate the finite element models for the multilayered honeycomb composite materials, in the linear elastic domain, the forces and displacements of the stamp are extracted for each of the four geometrical models.

Table 2

Finite element analysis results on multilayered honeycomb composite material with both cores impregnated

Displacement [mm]	Force [N] Model 1	Force [N] Model 2	Force [N] Model 3	Force [N] Model 4	Average force [N]
0.5	520.69	524.54	877.00	548.66	617.72
1	1041.40	1049.10	1754.00	1097.30	1235.45
1.5	1562.10	1573.60	2631.00	1646.00	1853.18
2	2082.70	2098.10	3508.00	2194.60	2470.85
2.5	2603.40	2622.70	4385.00	2743.30	3088.60

The value of the forces, for a given displacement of the stamp, is computed as an average of the reaction forces obtained for the four geometrical models for that displacement. The finite element simulation results are presented in the tables 2-5.

Table 3

Finite element analysis results on multilayered honeycomb composite material with the first core impregnated paper in the second paper

Displacement [mm]	Force [N] Model 1	Force [N] Model 2	Force [N] Model 3	Force [N] Model 4	Average force [N]
0.2	207.19	208.74	347.74	225.08	247.19
0.4	414.38	417.47	695.48	450.17	494.38
0.6	621.57	626.20	1043.20	675.25	741.56
0.8	828.76	834.94	1391.00	900.34	988.76
1	1035.90	1043.70	1738.70	1125.40	1235.93

Table 4

Finite element analysis results on multilayered honeycomb composite material with the first corer paper in the second impregnated paper

Displacement [mm]	Force [N] Model 1	Force [N] Model 2	Force [N] Model 3	Force [N] Model 4	Average force [N]
0.2	204.36	205.73	341.48	160.75	228.08
0.4	408.71	411.46	682.95	321.49	456.15
0.6	613.07	617.19	1024.40	482.24	684.23
0.8	817.43	822.92	1365.90	642.98	912.31
1	1021.80	1028.60	1707.40	803.73	1140.38

Table 5

Finite element analysis results on multilayered honeycomb composite material which both cores paper

Displacement [mm]	Force [N] Model 1	Force [N] Model 2	Force [N] Model 3	Force [N] Model 4	Average force [N]
0.1	101.62	102.31	169.18	106.99	120.03
0.2	203.24	204.61	338.37	213.98	240.05
0.3	304.86	306.92	507.55	320.96	360.07
0.375	381.08	383.65	634.44	401.21	450.10

7. Comparative analysis

To compare the experimental and finite element analysis results, force-displacement graphs were made for each material multilayered honeycomb

composite material configuration, in the linear elastic domain. These results are presented in Figs. 12-15.

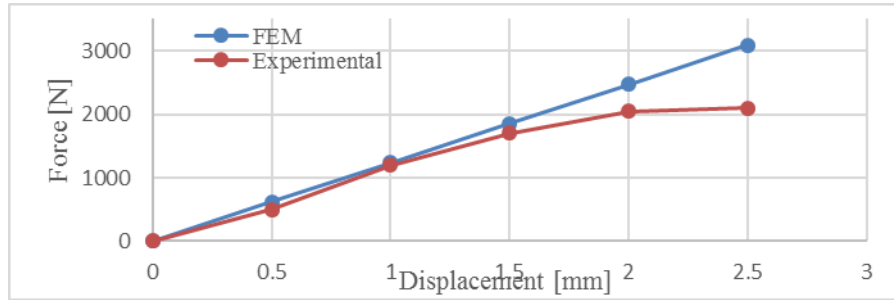


Fig. 12. Comparative analysis results on the first multilayered honeycomb composite material with both cores impregnated

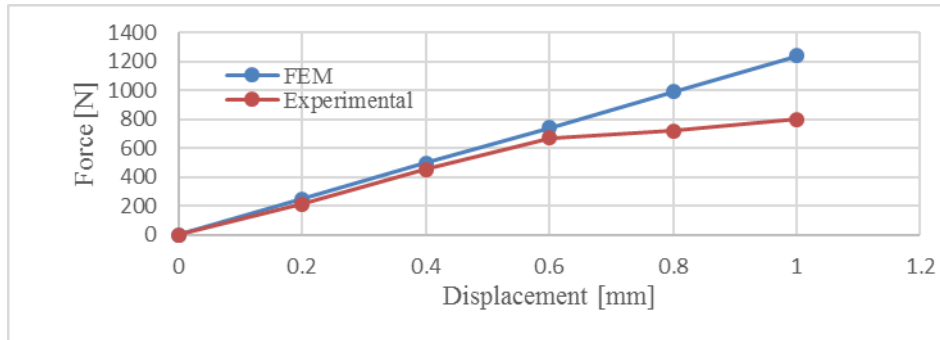


Fig. 13. Comparative analysis results on the second multilayered honeycomb composite material with the first core impregnated in the second paper

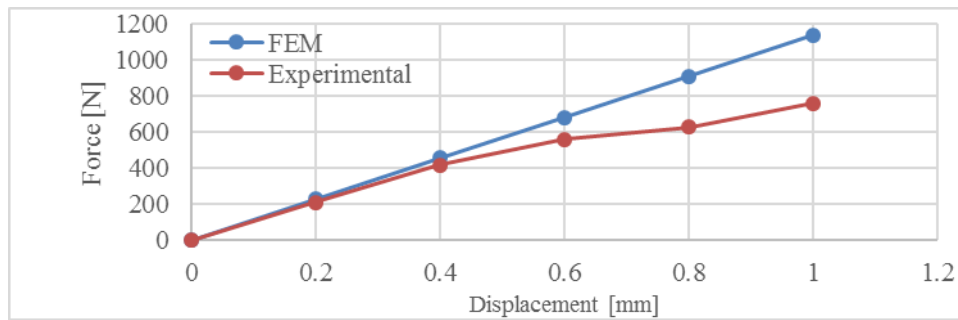


Fig. 14. Comparative analysis results on the third multilayered honeycomb composite material with the first corer paper in the second impregnated paper

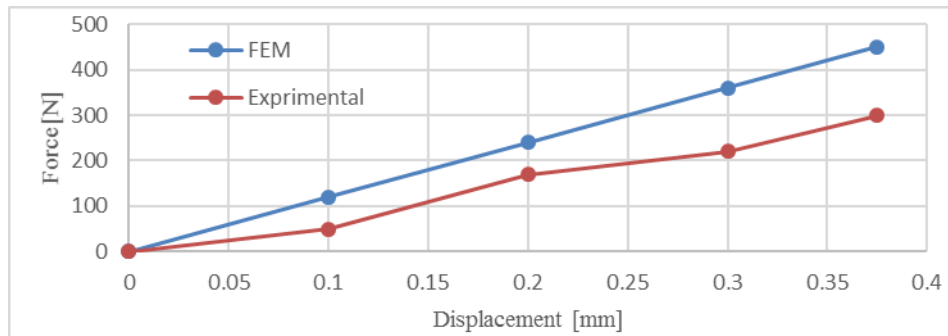


Fig. 15. Comparative analysis results on the fourth multilayered honeycomb composite material with both cores paper

8. Conclusions

The finite element models are validated in the linear elastic domain of the materials.

From the experimental results, it can be observed that the highest errors are obtained for the third and fourth multilayered composite material configurations. That is due to the fact that the natural mechanical properties of the paper are complex, and in the finite element model only the isotropic behavior of the paper was considered in the analysis.

The highest load capacity was obtained for the multilayered honeycomb composite material with boats cores impregnated.

The validation of these results allows finite element models to be used in determination of the behavior of multilayered honeycomb composite materials subjected to static loading in the linear elastic domain of the materials tested.

REFERENCES

- [1]. *L. J. Gibson, M. F. Ashby*, Cellular Solids Structure and Properties-Second Edition, 1988, USA;
- [2]. *P. Wriggers*, Computational Contact Mechanics, John Wiley and sons, 2002, USA;
- [3]. *J.R. Vinson*, The Behavior of Sandwich Structures of Isotropic and Composite Materials, Taylor & Francis Routledge, 1999;
- [4]. *A. Burr, J.B. Cheatham*, Mechanical Analysis and Design, Prentice-Hall, New Jersey, USA, 1995;
- [5]. *H.A. Petrescu*, Contributions to the Study of Behavior of Honeycomb Core Stratified Plates, Subjected to Static and Dynamic Loads, Bucharest, Romania, 2011;
- [6]. *R. Lakes*, Deformation Mechanism in Negative Poisson's Ratio Materials: Structural Aspects, Journal of material science, 1991;
- [7]. *E. F. Bruhn*, Analysis and Design of Flight Vehicles, Jacobs & Associated, 1965;
- [8]. *** ANSYS 14 User guide.

- [9]. *S.A. Galehdaria, M. Kadkhodayana, S. Hadidi-Mouda*, Analytical, Experimental and Numerical Study of Agraded Honeycomb Structure under In-Plane Impact Load with Low Velocity, *International Journal of Crashworthiness* Vol. 20, Iss. 4, 2015, pp. 387-400
- [10]. *C. Kassapoglou*, Stress Determination and Core Failure Analysis in Sandwich Rampdown Structures under Bending Loads, *Key Engineering Materials* 120-121 pp. 307-328, January 1996
- [11]. *T. Zhu, J. Chen, W. Gong*, Numerical Analysis of Debonded Honeycomb Sandwich Structure under Compressive Load, *Advanced Materials Research*, Vol 658, pp 227-231, Trans Tech Publications, Switzerland, 2013
- [12]. *M. Xihuia, M. Xiaoyub, Z. Xiaoyac*, Numerical Computation for Effective Mechanical Properties of Honeycomb Core Structure, *Advanced Materials Research*, Vol. 912-914, pp 460-465, Trans Tech Publications, Switzerland, 2014
- [13]. *A. Akatay, M.O. Bora, O. Coban, S. Fidan, V. Tuna*, The influence of low velocity repeated impacts on residual compressive properties of honeycomb sandwich structures, *Compos. Struct.* 125 (2015), pp. 425-433.
- [14]. *W. Abramowicz*, Thin-walled structures as impact energy absorbers, *Thin Wall. Struct.* 41 (2003), pp. 91-107.
- [15]. *N.K. Gupta, G.L. Easwara Prasad, S.K. Gupta*, Plastic collapse of metallic conical frusta of large semi-apical angles, *Int. J. Crashworthiness* 2 (1997), pp. 349-366.
- [16]. *A. Meran, C. Baykasoglu, A. Mugan, T. Toprak*, Development of a Design for a Crash Energy Management System for Use in a Railway Passenger Car, *Proc. Inst. Mech. Eng. F J. Rail Rapid Transit.* 230, 2016, pp. 206-219.
- [17]. *C.C. Foo, G.B. Chai, L.K. Seah*, Mechanical properties of Nomex material and Nomex honeycomb structure, *Composite Structures*, vol. 80, Elsevier, 2007, pp. 588-594.